DAMPING OF SINGLE-PARTICLE STATES AND GIANT RESONANCES IN ^{208}Pb

G.F. BERTSCH [1]
Cyclotron Laboratory, Michigan State University, East Lansing, MI 48824, USA

and

P.F. BORTIGNON [2], R.A. BROGLIA and C.H. DASSO [3]
The Niels Bohr Institute, University of Copenhagen, DK-2100 Copenhagen Ø, Denmark

Received 17 October 1978

The damping width of single-particle states and of giant resonances is estimated in ^{208}Pb, based on the excitation of surface modes and $T = 1$ pairs. The damping is dominated by the collectivity of the surface modes, with the pairing modes playing a weaker role. For both the single-particle states and giant resonances, the predicted damping is somewhat small. This could be due to the neglect of $T = 0$ particle–particle correlations or to the neglect of the volume modes. The damping for the giant resonances is reduced by the coherence between particle and hole.

A systematic description of the low-lying nuclear spectrum can be achieved for single- and doubly-closed shell nuclei in terms of surface and pairing vibrations, together with single nucleon degrees of freedom. This model has been very successful for nuclei in the neighborhood of ^{208}Pb, (cf. e.g. ref. [1]). The dominance of the surface degrees of freedom in the nuclear vibrations has been justified microscopically with the self-consistent RPA model [2]. A perturbation expansion can be constructed which explicitly displays these degrees of freedom and is in principle exact. This expansion, which we call Nuclear Field Theory (NFT) allows boson and fermion interactions through the two-body residual nuclear interaction and through particle–vibration couplings. The expansion parameter in the NFT approach to the nuclear many-body problem is $1/\Omega$, Ω being the effective degeneracy of the valence shells.

In the present paper we apply the NFT to the calculation of the width of single-particle states and of giant isoscalar resonances in ^{208}Pb. There is extensive literature on the theory of widths of single-particle states [3–9] and of giant vibrations [10–17]. However, these works do not treat the single-particle states and the giant vibrations together, and so do not reach firm conclusions on the validity of the models applied. By focussing on one quantity alone, the damping width, we shall show that existing theory accounts quite well for the relative magnitude of damping in single-particle states and in-vibrations, but falls short on absolute magnitudes.

In the NFT, the lowest-order contributions to the width of a single-particle state, Γ_p, are given by the imaginary parts of the self-energy graphs shown in fig. 1A–C,

$$\Gamma_p = 2\,[\mathrm{Im}\,(\Sigma_A - \tfrac{1}{2}\Sigma_C) + \mathrm{Im}\,\Sigma_B]\,. \qquad (1)$$

In graphs 1A and 1B, a particle is damped by bouncing inelastically off the nuclear surface, exciting a particle–hole or a pairing vibration. Graph 1C, which distinguishes the lowest-order NFT from other particle–vibration models, is necessary to correct for the miscounting of the exchange interaction in graph 1A [18]. To order $1/\Omega$ there is no corresponding correction to Σ_B. However, there is a graph of order $1/\Omega^2$ which is equivalent

[1] Supported by the National Science Foundation, Grant No. PHY-76-20097 A01.
[2] Present address: Istituto di Fisica Galileo Galilei, Padova, Italy; INFN Sez. Padova, Italy.
[3] Present address: Institut für Kernphysik, Heidelberg, West Germany.

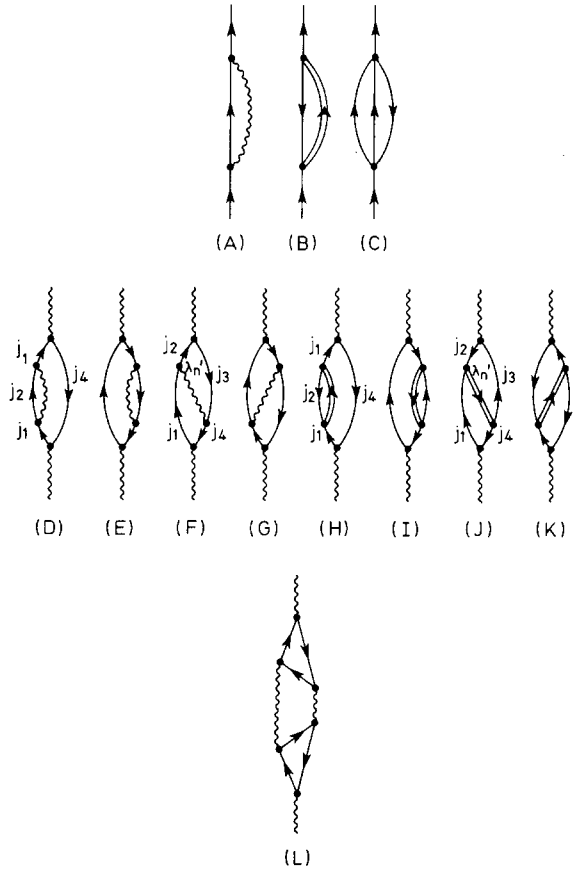

Fig. 1. Lowest-order $(1/\Omega)$ graphical NFT contributions to the width of single-particle and giant resonances. In (A)–(C) the lowest-order contributions to the single-particle widths are shown. A single-arrowed line represents a particle while a double-arrowed line indicates a pairing vibrational mode. A wavy line represents a surface vibration. The contributions to the width of the giant resonances utilized in the calculations are displayed in (D)–(K).

to graph 1C if the underlying force is the same for the particle–particle and particle–hole channels.

The analytic expression for graphs 1A or 1B is given by

$$\mathrm{Im}\,\Sigma(j) = \kappa^2 \sum_{\lambda n, j'} \frac{\beta_n^2(\lambda)}{(2\lambda+1)(2j+1)} \langle j \| r \frac{\partial U}{\partial r} Y_\lambda \| j' \rangle^2 \times \eta / [(\epsilon_j - \epsilon_{j'} - W_n(\lambda))^2 + \eta^2] ,$$

where

$$\langle j \| r \frac{\partial U}{\partial r} Y_\lambda \| j' \rangle = (-1)^{j+1/2} \int \phi_j \phi_{j'} \frac{\partial U}{\partial r} r^3 \mathrm{d}r \times \left[\frac{(2\lambda+1)(2j+1)(2j'+1)}{4\pi} \right]^{1/2} \begin{pmatrix} j & \lambda & j' \\ \frac{1}{2} & 0 & -\frac{1}{2} \end{pmatrix} . \quad (2)$$

The various quantities appearing in this equation are defined as follows. The $\beta_n(\lambda)$ is the deformation parameter associated with the nth phonon of multipolarity λ[‡1]. The function $U(r)$ is the shell model potential which determines the single-particle states; for the particle–hole interaction we use a Woods–Saxon form with $V_0 = 50$ MeV, $r_0 = 1.25$ fm and $a = 0.65$ fm. The energy of the phonon is denoted by $W_n(\lambda)$, and η is an averaging parameter, taken to be 0.5 MeV. Finally, κ is a coupling strength which ought to be equal to 1 in a self-consistent theory. Calculations of damping of single-particle motion based on eq. (2) have been carried out many times in the past [6–9], with various assumptions about the β-moments.

We shall determine the particle–hole β-moments with the RPA theory, which can be adjusted to describe known excitations, and then gives reliable predictions for the remainder of the strength. When using the RPA β-moments, it is not necessary to explicitly sum over eigenstates. Instead we use the imaginary part of the Green's function directly. This is related to the sum over β-moments as follows:

$$\sum_n \frac{\beta_n^2(\lambda)}{(2\lambda+1)} \frac{\eta}{(\epsilon - W_n)^2 + \eta^2} = \mathrm{Im}\, G_\lambda^{\mathrm{cor}}(\epsilon + \mathrm{i}\eta) \equiv \mathrm{Im}\, G_\lambda^0(\epsilon + \mathrm{i}\eta) / [1 + \kappa V_0 \rho_0 f G_\lambda^0(\epsilon + \mathrm{i}\eta)] , \quad (3)$$

where

$$G_\lambda^0(\omega) = \sum_{j,j'} \frac{\langle j \| r(\partial U/\partial r) Y_\lambda \| j' \rangle^2}{\rho_0^2 V_0^2 f^2} \frac{1}{(2\lambda+1)} \times ([\epsilon_j - \epsilon_{j'} - \omega]^{-1} + [\epsilon_j - \epsilon_{j'} + \omega]^{-1}) , \quad (4)$$

and $f = V_0^{-2} \int (r\, \partial U/\partial r)^2 r^2 \mathrm{d}r$. The sum in eq. (4) is over particles j and holes j'.

In the actual calculation, we used single-particle wavefunctions and energies from a Hartree–Fock theory with the Skyrme I interaction, but the eigenfunctions of a Woods–Saxon well would have served as well. The

[‡1] In the NFT language, the particle–vibration coupling strength is given by $\Lambda_n(\lambda) = \beta_n(\lambda)/(2\lambda+1)$.

parameter κ was chosen to put the $\lambda = 1$ vibration at zero energy. With $\rho_0 = 0.16\,\mathrm{fm}^{-3}$, this requires $\kappa = 1.6$, which is larger than the nominal value of 1. However, this is to be expected in any simple model in which both the transition density and the transition potential are described by the same function. The model reproduces the properties of the low-lying vibrations adequately enough for our purposes.

The pairing vibrations are described with a similar theory, except that $G^{(0)}$ is now given by

$$G_\lambda^{(0)}(\omega) = \sum_{j \geq j'} \frac{\langle j \| r(\partial U/\partial r) Y_\lambda \| j' \rangle^2}{V_0^2 \rho_0^2 f^2 (1 + \delta_{jj'})} (\epsilon_j + \epsilon_{j'} \pm \omega)^{-1}, \quad (5)$$

where the sum is over particle pairs and hole pairs. The sign in the energy denominator is negative for particles and positive for holes for the pair addition mode and vice versa for the pair removal mode. The pairing interaction strength is taken to be the same as the strength of the particle–hole interaction. This yields matrix elements close to those of the pairing multipole interaction of ref. [19]. However, the lowest pair states in the present model tend to be less correlated than is found empirically, due to deficiencies in the single-particle spectrum of the Skyrme hamiltonian. Thus, it is likely that we underestimate the contribution of the pairing channel.

In the numerical results, we find that graph 1A dominates the self-energy width. This may be seen in table 1, where the contributions to single-particle widths are displayed. The dominance of graph 1A is understandable in view of the enormous effect that the RPA has on the particle–hole strength function. In the region of 3–6 MeV excitation, the $\mathrm{Im}\,G^{\mathrm{cor}}$ typically exceeds $\mathrm{Im}\,G^{(0)}$ by a factor of 10. We evaluate graph 1C by replacing G^{cor} by $G^{(0)}$, so it is evident that its effect is small.

Table 1
Damping of single-particle states in ^{208}Pb. The contributions associated with the diagrams A and B displayed in fig. 1 are given.

Orbit	Excitation energy	1A	1B	Γ_p (MeV)	
				theory	empirical
particles					
$s^{\nu}_{1/2}$	6.7	3.0	0.1	3.1	3.0–5.0 [20–22]
$d^{\nu}_{3/2}$	6.4	2.8	0.1	2.9	
$i^{\pi}_{11/2}$	8.2	1.5	0.1	1.6	
holes					
$h^{\nu}_{11/2}$	8.2	1.9	0.3	2.2	3.5 [23]
$g^{\pi}_{7/2}$	3.9	0.5	0.0	0.5	
$g^{\pi}_{9/2}$	6.9	1.7	0.1	1.8	

In examining the partial contributions to Σ_A, we find that in all cases no single state contributes more than 20% to the total width. This is important to ascertain, in that Γ may only be interpreted as a width if it is not dominated by a single intermediate state. Also the width depends only weakly on the precise value of η used in the averaging when many states contribute.

The calculated single-particle widths of table 1 can be compared with experiment in two ways. First, we can compare the imaginary self-energy of an orbit with the diagonal matrix elements of an empirical optical potential. Optical potentials fit to low energy s-wave neutron scattering [20–22] give expectation values somewhat higher than theory, as is shown in the last column. Information on the damping could also come from the direct observation of a width of a single-particle state populated by a transfer reaction. In the case of ^{207}Pb, the $h^{\nu}_{11/2}$ strength can be identified because of its high angular momentum, and its damping width measured [23]. Again the empirical width is larger than the theoretical. One possible reason for this discrepancy is that we neglected the vibrations of the nuclear interior and the spin–isospin modes. Certainly at higher energies, the dominant damping must be from the volume modes. Jeukenne et al. [24] account for the empirical optical potential using a Fermi gas model of the nucleus for which most of the absorption takes place in the interior. We intend to examine this paradox between the different treatments in a future publication. Another possible explanation for the discrepancy is that we neglected the $T=0$ pairing channel. Satchler and collaborators [6,25] in their study of the proton optical potential at higher energies, find the deuteron channel to be of comparable importance to the inelastic excitation channels.

It is of interest to plot the damping width of an orbit, considering its excitation energy as an independent variable, to compare with simple models for the dependence of the damping on energy. This is shown in fig. 2 for the $s^{\nu}_{1/2}$ orbit. We see that there is a rather sudden onset of damping at $E \approx 5$ MeV, and that the damping

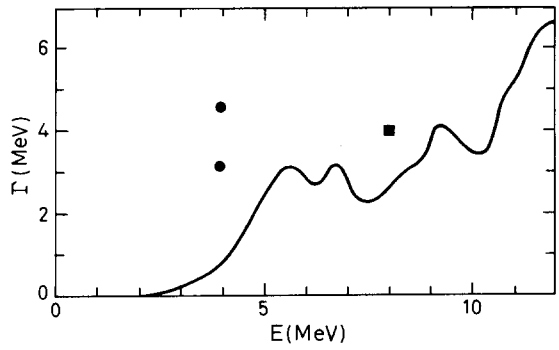

Fig. 2. Width of $s^{\nu}_{1/2}$ state in ^{209}Pb, as a function of excitation energy of the state. The dots and square indicate the width from empirical optical potential fit to s-wave neutron strength function [21,22] and to neutron scattering [23], respectively.

is roughly constant between 5 and 10 MeV. This behavior arises from the dominant role of the surface vibrations and is at variance with the E^2 dependence predicted by the Fermi gas model.

We now turn to the damping of giant vibrations. Previous microscopic calculations of this damping under various assumptions include refs. [13–17]. From our experience with the single-particle damping, we know that the only important graphs are ones with intermediate phonons, and we restrict ourselves to these graphs. The graphs including a single intermediate phonon are shown in fig. 1D–1K. There is one more graph which may be significant that we have not yet calculated, the two-phonon graphs shown in fig. 1L. Some calculations including two-phonon states are reported in ref. [16].

Graphs 1D, E, H and I are directly analogous to the single-particle damping: a particle or hole in the vibration independently excites a phonon. The expression for the width arising from these graphs is

$$\Gamma_{\rm vib}(\lambda_n) = 2\kappa^2 \sum_{\substack{j_1 j_2 j_4 \\ n'\lambda'}} \frac{\beta^2_{n'}(\lambda') X^2_n(j_1 j_4;\lambda)}{(2\lambda'+1)(2j_1+1)} \times \langle j_1 \| r \frac{\partial U}{\partial r} Y_{\lambda'} \| j_2 \rangle^2 \times \eta / [(W_n(\lambda) - W_{n'}(\lambda') - \epsilon_{j_2} + \epsilon_{j_4})^2 + \eta^2] , \quad (6)$$

where

$$X_n(j_1 j_4;\lambda) = \Lambda_n \frac{\langle j_1 \| r(\partial U/\partial r) Y_\lambda \| j_4 \rangle}{W_n(\lambda) - \epsilon_{j_1} + \epsilon_{j_4}} ,$$

is the amplitude of the state $|j_1 j_4\rangle$ in the vibration. The j_i sums are restricted to particles or holes according to the directions of the arrows in the graphs. We include all time orderings of the graphs which contain one intermediate phonon. If graphs 1D, E, H and I were the only important graphs, the damping of the vibration could be related directly to the single-particle damping, as was assumed in ref. [11]. However, the graphs 1F, G, J and K, involving the exchange of a phonon, act to suppress the damping. Qualitative arguments have been made for this behavior by Bertsch [10] and by Ui [12], and have been found to have some validity in light nuclei [14]. The reason for the suppression is that a collective vibration has static properties close to the ground state; the particle and hole tend to act with opposite signs on an external probe, or in our case, on the intermediate phonon. The expression for graph 1F or 1G is

$$\Gamma_{\rm vib}(\lambda_n) = 2\kappa^2 \sum_{\substack{j_1 j_2 j_3 j_4 \\ n'\lambda'}} (-1)^{j_4 - j_1 + \lambda + \lambda'} \frac{\beta^2_{n'}(\lambda')}{2\lambda'+1} \times X_n(j_1 j_4;\lambda) X_n(j_2 j_3;\lambda) \times \frac{\langle j_4 \| r(\partial U/\partial r) Y_{\lambda'} \| j_3 \rangle \langle j_2 \| r(\partial U/\partial r) Y_{\lambda'} \| j_1 \rangle \eta}{(W_n(\lambda) - W_{n'}(\lambda') - \epsilon_{j_1} + \epsilon_{j_3})^2 + \eta^2} \times \begin{Bmatrix} j_1 & j_2 & \lambda' \\ j_3 & j_4 & \lambda \end{Bmatrix} . \quad (7)$$

We calculate the damping of the monopole and quadrupole giant resonances with eqs. (6) and (7). The energy of the quadrupole is taken at the empirical value 10.9 MeV, which is close to the result of the self-consistent theory. The energy of the monopole is sensitive to the interaction in the nuclear interior, which is not as well known as the surface interaction. The self-consistent Skyrme theories place the state at $\approx$18 MeV, but recent experimental evidence favours 13.9 MeV, and we use this value for our calculation. It is worth noting that the state is extremely collective at this energy, in the sense that the wavefunction is thoroughly divided over many particle–hole components. The results for the damping are shown in table 2. In both cases many intermediate states contribute significantly to the total width. The largest single contribution amounts to less than 10% of the total width. The analysis of the width by graph in table 2 shows

Table 2
Damping of isoscalar resonances in ^{208}Pb. The contributions associated with the different diagrams displayed in fig. 1 are given.

	1D, E	1F, G	1H, I	1J, K	Γ (MeV)	
					theory	experiment [26]
2^+	4.15	−1.81	0.09	0.0	2.43	3.0±0.3
0^+	1.10	−0.30	0.20	−0.18	0.82	2.5±0.6

that the exchange graph has the opposite sign as expected, decreasing the total width substantially. The experimental widths of the giant resonances, quoted in the last column of table 2, are larger than calculated. The discrepancy is somewhat worse than for the single particle states. As with the single-particle states, inclusion of $T = 0$ pairs and the volume modes of vibration, and a better treatment of $T = 1$ pairs, might significantly increase the damping. In addition, the two-phonon graph ought to increase the damping of the vibrations as well. Calculations of this graph are now in progress.

One of the authors (G.B.) would like to thank G. Richter for help on the numerical calculations.

References

[1] P.F. Bortignon, R.A. Broglia, D.R. Bes and R. Liotta, Phys. Rep. 30C (1977) 305.
[2] G. Bertsch and S.F. Tsai, Phys. Lett. 50B (1974) 319.
[3] B. Block and H. Feshbach, Ann. Phys. 23 (1963) 49.
[4] C. Shakin, Ann. Phys. 22 ((1963) 373.
[5] M. Divadeenam, W. Beres and H. Newson, Ann. Phys. 69 (1972) 428.
[6] C.L. Rao, M. Reeves and G.R. Satchler, Nucl. Phys. A207 (1973) 182.
[7] A. Lev, W. Beres and M. Divadeenam, Phys. Rev. Lett. 31 (1973) 555.
[8] T.F. O'Dwyer, M. Kawai and G.E. Brown, Phys. Lett. 41B (1972) 259.
[9] V.G. Soloviev and L.A. Malov, Nucl. Phys. A196 (1972) 433.
[10] G. Bertsch, Phys. Lett. 37B (1971) 470.
[11] C. Dover, R. Lemmer and F. Hahne, Ann. Phys. 70 (1972) 458.
[12] H. Ui, Proc. Conf. on New giant resonances (Sendai, Japan, 1975) p. 105.
[13] M. Danos and W. Greiner, Phys. Rev. B138 (1965) 876.
[14] T. Hoshino and A. Arima, Phys. Rev. Lett. 37 (1976) 266.
[15] J.H. Dehesa et al., Phys. Rev. C15 (1977) 1858.
[16] V.G. Soloviev, C. Stoyanov and A. Vdovin, Nucl. Phys. A288 (1977) 376.
[17] S. Adachi and S. Yoshida, Nucl. Phys., to be published.
[18] D. Bes et al., Nucl. Phys. A260 (1976) 84.
[19] R.A. Broglia, D.R. Bes and B.S. Nilsson, Phys. Lett. 50B (1974) 213.
[20] P.A. Moldauer, Nucl. Phys. 47 (1963) 65.
[21] P.A. Moldauer, Nucl. Phys. 47 (1963) 65.
[21] S.F. Mughabghab and D. Garber, Neutron cross sections (BNL 325, Brookhaven National Lab., 1973) Vol. I, p. xx.
[22] L. Cranberg et al., Phys. Rev. 159 (1967) 969.
[23] S. Galès, private communication.
[24] J. Jeukenne, A. Lejeune and C. Mahaux, Phys. Rep. 25C (1976) 83.
[25] P.W. Coulter and G.R. Satchler, Nucl. Phys. A293 (1977) 269.
[26] M. Harakeh et al., Phys. Rev. Lett. 38 (1977) 676.